

1 **Prediction of ‘Nules Clementine’ mandarin susceptibility to rind breakdown**  
2 **disorder using Vis/NIR spectroscopy.**

3

4 **ABSTRACT**

5 The use of diffuse reflectance visible and near infrared (Vis/NIR) spectroscopy was  
6 explored as a non-destructive technique to predict ‘Nules Clementine’ mandarin fruit  
7 susceptibility to rind breakdown disorder (RBD) by detecting rind physico-chemical  
8 properties of individual intact fruit from different canopy positions. Vis/NIR spectra were  
9 obtained using a LabSpec® spectrometer. Reference physico-chemical data of the fruit  
10 were obtained after 8 weeks of storage at 8°C using conventional methods and included  
11 RBD, H°, colour index, fruit mass loss, rind dry matter, sugar (sucrose, glucose, fructose,  
12 total sugars), phenolic acid concentrations. Principal component analysis (PCA) was  
13 applied to analyse spectral data to identify clusters in the PCA score plots and outliers.  
14 Partial least squares regression (PLSR) was applied to spectral data after PCA to develop  
15 prediction models for each quality attribute. The spectra were subjected to a test set  
16 validation by randomly dividing the data into calibration (60%) and validation (40%)  
17 sets. PLS-discriminant analysis (PLS-DA) models were developed to sort fruit based on  
18 canopy position and RBD susceptibility. Fruit position within the canopy had a  
19 significant influence on rind biochemical properties. Outside fruit had higher rind sugar,  
20 phenolic acids and dry matter content and lower RBD index than inside fruit. The data  
21 distribution in the PCA and PLS-DA models displayed four clusters that could easily be  
22 identified. These clusters allowed distinction between fruit from different preharvest  
23 treatments. NIR calibration and validation results demonstrated that sugars, dry matter,

24 colour index and mass loss were predicted with significant accuracy. The good  
25 correlation between spectral information and sugar content demonstrated the potential of  
26 Vis/NIR as a non-destructive tool to predict fruit susceptibility to RBD.

27

28 Keywords: Non-destructive technique · Vis/near infrared spectroscopy · Rind breakdown  
29 disorder (RBD) · Citrus · ‘Nules Clementine’ Mandarin · Canopy position.

30

## 31 **1. Introduction**

32

33 South Africa produces approximately 100 000 tons of Clementine mandarins per annum,  
34 making it the third largest producer and exporter of Clementine mandarins in the world  
35 after Spain and Morocco ([Barry and Rabe, 2004](#)). The development of various types of  
36 physiological disorders limits the postharvest storage capability and causes commercial  
37 losses. A lack of understanding the physiological mechanism underlying these disorders  
38 affects both supply and profits. The challenge is significant regarding rind breakdown  
39 disorder (RBD) of ‘Nules Clementine’ mandarins (*Citrus reticulata* Blanco.) that do not  
40 manifest during harvest grading and postharvest treatments but develop about 3 to 5  
41 weeks after harvest.

42

43 RBD is initially manifested on the equatorial plane as small, irregular, slightly sunken  
44 and colourless patches of about 3 to 6 mm in diameter scattered about the flavedo (the  
45 outer-most, pigmented part of citrus rind) of the fruit ([Cronje et al., 2011](#)). These sunken  
46 areas, occurring directly above and among the oil glands of the flavedo, coalesce

47 producing larger affected areas, turning redish-brown to dark-brown, become dry and  
48 necrotic in the severe stages of the disorder with extended storage period (Cronje, 2007,  
49 2009). According to Agustí et al. (2001) browning of affected rind surface appears to be  
50 the result of oxidative processes.

51

52 Intensive research has been conducted towards determining factors triggering RBD. As a  
53 result, it has been established by several research groups that different microclimates are  
54 influencing sensitivity of fruit to RBD and similar rind disorders such as rind pitting on  
55 oranges (Alferez and Zacarias, 2001) and grapefruit (Alferez and Burns, 2004) and peteca  
56 spots on lemons (Wild, 1991). In a study conducted in Spain (northern hemisphere),  
57 Almela et al. (1992) reported that these fluctuations could also be observed among fruits  
58 from the same tree and the incidence being by exposure of individual fruit to the sun.  
59 These investigators further showed that fruit oriented to the north-west (NW) in canopy  
60 were most affected by the disorder. In a later study conducted in the same country, Agustí  
61 et al. (2001) corroborated that fruit positioned in the NW face of the tree to be more  
62 prone to develop the rind pitting disorder and this was reported to be consistent over five  
63 seasons. Similar observations were reported in ‘Fortune’ (Duarte and Guardiola, 1995)  
64 and ‘Encore’ (Chikaizumi, 2000) mandarin fruit, where it was maintained that the  
65 disorder affects mainly the exposed fruit from the north-west quadrant of the tree.

66

67 In a study conducted in South Africa (southern hemisphere), fruit position, and therefore  
68 exposure to high (outside) or low (inside) light levels in the canopy, affect the flavedo  
69 concentration of carbohydrates during fruit development (Cronje, 2009; Cronje et al.

70 [2011](#)). The latter authors reported the flavedo from fruit borne on the outside of the  
71 canopy to have significantly higher sucrose, glucose and fructose content than the fruit  
72 borne inside the canopy. Interestingly, the results obtained by this group of investigators  
73 revealed a correlation between fruit position, rind sugar content and ultimately  
74 development of RBD. The incidence of rind breakdown was higher on inside fruit  
75 compared with the outside fruit and this was consistent from season to season and could  
76 be attributed to their exclusion from adequate sunlight during their fruit development. In  
77 addition, fruit borne inside the canopy had lower chlorophyll and carotenoid contents,  
78 and therefore poorer rind colour ([Khumalo, 2006](#)), and lower carbohydrates rendered  
79 them susceptible to the disorder ([Cronje, 2009](#)). Although intensive research aimed at  
80 appreciating RBD has been conducted, the disorder still occurs frequently and  
81 unpredictably, reducing the quality of the fruit ([Almela et al., 1992](#); [Cronje, 2005](#)).

82

83 There is therefore a need to develop an objective, fast and non-destructive assessment  
84 that can be used to determine/predict citrus fruit susceptibility to rind disorders  
85 accurately. Non-visible information, such as that provided by near infrared (NIR) region  
86 of the spectrum can improve the inspection by detecting rind biochemical profile and  
87 hence the detection of non-visible physiological disorders ([Blasco et al., 2007](#)). Most  
88 current non-destructive quality measurement using NIR spectroscopy (NIRS) has been  
89 developed to assess fresh fruit according to their internal quality attributes ([Butz et al.,](#)  
90 [2005](#)). Very limited research work has been conducted to develop a technology that can  
91 assess, predict and monitor the physiological disorders and rind physiological disorders  
92 of citrus fruit in particular. Nevertheless, NIRS has been used successfully to detect

93 surface bruising in apple (Geeola et al., 1994), surface defects in peach (Miller and  
94 Delwiche, 1991), storage disorders in kiwifruit (Clark et al., 2004) and drying internal  
95 disorder in Tangerine citrus (Peiris et al., 1998). Recently, Teerachaichayut and co-  
96 workers (2011) successfully used NIR spectroscopy to non-destructively predict pericarp  
97 hardening disorder in magosteen fruit. The trend has constantly shifted towards  
98 developing reliable and cost effective technologies to non-destructively screen fruit  
99 physiological disorders. Recently, Zheng et al. (2010) used NIR in the reflectance mode  
100 to predict oleocellosis sensitivity in citrus fruit. A review by Magwaza et al. (2011)  
101 discusses the recent developments and application of Vis/NIR spectroscopy to non-  
102 destructively evaluate internal and external fruit quality.

103

104 In summary, the knowledge of biochemical changes in the rind of citrus fruit that could  
105 be used to precisely predict fruit rind condition and therefore susceptibility to rind  
106 disorders is limited. However, previous research by Cronje et al. (2011) indicated that  
107 fruit position within the canopy affects rind biochemical profile, particularly  
108 carbohydrate concentration and hence susceptibility of fruit to RBD. This study aims to  
109 explore the use of diffuse reflectance Vis/NIR spectroscopy in the wavelength range of  
110 350-2500 nm as a non-destructive tool to predict susceptibility to RBD by detecting rind  
111 physico-chemical properties of individual intact fruit from different canopy positions.

112

## 113 **2. Material and methods**

114

115 2.1. *Site, fruit sampling and postharvest handling*

116

117 A total of 15 ‘Nules Clementine’ mandarin trees in an orchard at Stellenbosch University  
118 experimental farm, Western Cape Province, South Africa (33°53’4.56”S, 18°37’36.84”E)  
119 were identified and marked based on their health and fruit setting ability. On each tree,  
120 200 fruit from sun-exposed and 200 from shaded canopy positions were randomly  
121 selected and tagged. To increase our success of having fruit with RBD, a method of  
122 enhancing the disorder demonstrated by Cronje (2009) was adopted. Briefly, during  
123 January 2011 (after physiological drop about four months until commercial maturity),  
124 half of the selected fruit from each position was covered with brown paper bags without  
125 removing or covering subtending leaves. The study consisted of four preharvest  
126 treatments, viz., outside, outside bagged, inside and inside bagged.

127

128 Upon reaching commercial maturity, on 16 May, individual fruit were harvested  
129 according to industry practice, coded according to treatment and canopy position and  
130 underwent all commercial postharvest practices, including drenching (Thiabendazole, 500  
131 mg/L; Imazalil, 500 mg/L and 2,4-dichlorophenoxyacetic acid, 125 mg/L) and waxing  
132 (polyethylene citrus wax, Citrushine®, Johannesburg, South Africa). After which they  
133 were brought to the postharvest evaluation laboratory, sorted to remove any defective  
134 fruit and weighed. A total of 80 blemish free fruit (20 fruit from each treatment) were  
135 selected to provide fruit samples for non-destructive and destructive measurements. After  
136 phytosanitary inspection and certification, these fruit were separately packed in boxes

137 marked, sent at room temperature via a courier service to Cranfield University (CU) in  
138 the United Kingdom, where postharvest storage took place.

139

## 140 2.2. *Spectral acquisition*

141

142 Vis/NIR spectra were obtained upon arrival at CU using a method described by Kuang  
143 and Mouazen (2011). Spectral acquisition from intact fruit samples was carried out using  
144 a mobile fibre-optic Vis/NIR spectrophotometer (350-2500nm) (LabSpec2500(r) Near  
145 Infrared Analyzer, Analytical Spectral Devices Inc., USA) in diffuse reflectance mode  
146 equipped with one Si array (350-1000nm) and two Peltier cooled InGaAs detectors  
147 (1000-1800 nm and 1800-2500 nm). The sampling interval of the instrument was 1 nm.  
148 However, the spectral resolution was 3 nm at 700 nm and 10 nm at 1400 nm and 2100  
149 nm. A high intensity probe with an in-built light source was used. A quartz-halogen bulb  
150 of 3000 Kelvin light source and a detection fibre are gathered in the high intensity probe  
151 enclosing a 35° angle.

152

153 Prior to scanning the fruit samples, and periodically at intervals of 30min, white reference  
154 measurements were taken. Fruit samples were placed in direct contact with the high  
155 intensity probe. Reflectance spectral data was acquired from 8 position of the fruit; 4  
156 from equatorial spots of the fruit and 2 from the stem-end and 2 from the stylar-end of the  
157 fruit, averaged and used for spectral pre-processing and multivariate analysis.

158

159 2.3. *Physico-chemical measurements to obtain reference values*

160

161 2.3.1. *Storage conditions, RBD rating, weight and rind colour*

162

163 After scanning, fruits were stored in a cold room with delivery air temperature of 8°C, a  
164 temperature which is known to cause the highest degree of RBD incidence (Khumalo,  
165 2006). During cold storage, fruit were scored weekly, for the incidence of RBD for the  
166 duration of 8 weeks. RBD was scored on a subjective scale from 0 = no breakdown to 3 =  
167 severe breakdown. RBD was then expressed as RBD index (RBDI), estimated as  
168 previously described (Alferez et al., 2003) and calculated according to the following  
169 formula previously reported for chilling injury and peel pitting by Lafuente et al. (1997)  
170 and Lafuente and Sala (2002):

171

$$172 \quad RBDI = \frac{\sum \{RBD(0-3) \times \text{No. of fruit in each class}\}}{\text{Total number of fruit}} \quad (1)$$

173

174 Fruit were weighed weekly using a calibrated balance (Mettler Toledo, ML3002E / 01,  
175 Switzerland). Rind colour components were measured in L\*a\*b\* colour space using  
176 Minolta CR-400 colourimeter (Chroma Meter CR-400, Konica Minolta Sensing Inc.,  
177 Japan) after calibration using standard white tile (CR-A43; Y = 93.1, x = 0.3138; y =  
178 0.3203). From L\*, a\* and b\* colour parameters, colour index (CI) was calculated  
179 according to Jimenez-Cuesta et al. (1981) using the following formula:

180



181  $CI = \frac{1000 \times a}{L \times b}$  (2)

182

183 *2.3.2. Sample preparation*

184

185 After 8 weeks in storage, fruit samples were destructed where rind was peeled from the  
186 rest of the fruit. The pulp was juiced and the juice used for fresh TSS analysis. TSS was  
187 measured with a digital hand-held refractometer (Palette, PR-32 $\alpha$ , Brix 0.0-32.0, Atago,  
188 Co. LTD, Japan) using 1 mL of freshly squeezed juice and expressed as °Brix. The rind  
189 from each sample was snap frozen in liquid nitrogen, separated into two portions, of  
190 which one portion was stored at -40°C and the other at -80°C freezer until further  
191 analysis.

192

193 Fresh frozen rind samples were freeze-dried in Edwards Modulyo freeze drier (W.  
194 Sussex, UK) for 7 days at 0.015 kPA and -55°C. Lyophilized samples were weighed and  
195 water content was calculated from freeze dried samples and expressed as a percentage of  
196 fresh weight. Samples were then ground using pestle and mortar into fine powder and  
197 returned into the freezer prior to being used for sugar and phenolic acids determination by  
198 HPLC.

199

200 *2.3.3. Extraction and HPLC quantification of non-structural sugars*

201

202 Sugar was extracted from 150 mg of fruit rind powder using 62.5% (v/v) aqueous  
203 methanol as described elsewhere by [Terry et al. \(2007\)](#). Following extraction,

204 concentration of fructose, glucose and sucrose was determined using an Agilent 1200  
205 series HPLC binary pump system (Agilent, Berks., UK), equipped with an Agilent  
206 refractive index detector (RID) G1362A, based on the method described by [Crespo et al.](#)  
207 [\(2010\)](#). Briefly, sample extracts was diluted (1:10), and injected into a Rezex RCM  
208 monosaccharide Ca<sup>+</sup> (8%) column of 300 mm x 7.8 mm diameter (Phenomenex,  
209 Torrance, CA) with a Carbo-Ca<sup>2+</sup> guard column of 4 mm x 3 mm diameter  
210 (Phenomenex). Temperature of the column was set at 80°C using a G1316A  
211 thermostated column compartment. The mobile phase used was HPLC-grade water at a  
212 flow rate of 0.6 ml/min ([Giné Bordonaba and Terry, 2008](#)). The presence and abundance  
213 of the selected sugars was calculated by comparison of peak area with peak of known  
214 standards using ChemStation Rev. B.02.01.

215

#### 216 *2.3.4. Extraction and HPLC quantification of phenolic compounds*

217

218 Phenolic acids were extracted and quantified using a method described elsewhere by  
219 [\(Magwaza et al., 2012\)](#). Briefly, a 150 mg of freeze dried rind powder was dissolved into  
220 3 mL 70:29.5:0.5 (methanol:H<sub>2</sub>O:HCL). Samples were extracted at 35°C in water bath  
221 for 30 minutes, agitated for 30s every 5 minutes and the flocculate filtered through a 0.2  
222 µm syringe filter. Phenolic acid concentrations were determined using the HPLC system  
223 equipped with an Agilent DAD G1315B/G1365G photodiode array with multiple  
224 wavelength detector.

225

226 2.3.5. *Determination of antioxidant capacity*

227

228 Antioxidant capacity was measured on freeze-dried samples following the method by  
229 [Crespo et al. \(2010\)](#). The absorbance of prepared sample solutions was measured  
230 spectrophotometrically at 517 nm using a Camspec M501 UV/vis spectrometer.  
231 Basically, the antioxidant capacity determination with 2,2-diphenyl-1-picrylhydrazyl  
232 (DPPH) is based on the properties of DPPH, which its radical form has an absorption  
233 band at 517 nm and disappears upon reduction by an antiradical compound.

234

235 2.4. *Data analysis*

236

237 2.4.1. *Statistical analysis*

238

239 Statistical analyses carried out using SPSS 10.0 for Windows (SPSS Inc. Chicago, USA).  
240 Data was subjected to analysis of variance (ANOVA). Least significant difference values  
241 (LSD; P=0.05) were calculated for mean separation ([Landahl et al., 2009](#)).

242

243 2.4.2. NIRS analysis, calibration development and validation

244

245 Before analysis, the reflectance spectra in Indico format (Indico Pro 5.6 software,  
246 Analytical Spectral Devices Inc., USA) were transformed to absorbance ( $\log(1/R)$ ).  
247 Calculations of the average of 8 spectra obtained from each fruit, pre-processing and

248 calibration methods were executed using the Unscrambler chemometric software (The  
249 Unscrambler Version 9.2, Camo Process, SA, Trondheim, Norway).

250

251 Several pre-processing methods including, smoothing using moving average and  
252 Savitzky-Golay methods, full multiple scatter correction (MSC), Savitzky-Golay first  
253 derivative and second derivative, minimum and maximum normalisation and vector  
254 normalisation (SVN) were tested to correct light scatter and reduce the changes of light  
255 path length. After pre-processing trials, the optimal model performance was obtained  
256 using the Savitzky-Golay second derivative with the polynomial order of 5 and MSC.  
257 Savitzky-Golay second derivative was used to correct light scattering properties while  
258 MSC was used to correct for additive, multiplicative effects of the spectra, and pathlength  
259 variations ([Leonardi and Burns, 1999](#); [Gómez et al., 2006](#)).

260

261 In order to determine effective wavelength, discriminate fruit from four canopy positions  
262 using Vis/NIR and to detect outliers, PCA was performed using full cross validation.  
263 Partial least squares regression (PLSR) was applied to spectral data to develop prediction  
264 models for each quality attribute. A PLS variant known as partial least squares  
265 discriminant analysis (PLS-DA) was also used in order to classify fruit from different  
266 canopy positions according to the spectra. A method by [Chen et al. \(2011\)](#) was used in  
267 the application of PLS-DA. Briefly, fruit from each of the canopy positions in the  
268 calibration set was assigned a dummy variable as a reference value (outside = 1, outside  
269 bagged = 2, inside = 3 and inside bagged = 4). In addition, due to discrete nature of RBD  
270 scores, samples were assigned a binary dummy variable as a reference value, which was

271 an arbitrary number whether the sample belongs to a particular position or not. RBD  
272 affected fruit were set as reference data one, while unaffected fruit were assigned to 1  
273 ([Teerachaichayut et al., 2011](#)).

274

275 To develop PLS models, the dataset was randomly separated into two subsets, 60% for  
276 calibration and 40% for test set validation. The regression statistics of developed models  
277 was described by the value of the root mean square error of calibration (RMSEC), root  
278 mean square error of validation or prediction (RMSEP), the Pearson correlation  
279 correlation coefficients (R) between predicted and observed reference values, number of  
280 latent variables (LVs), and the residual predictive deviation (RPD), described by  
281 [Williams and Sobering \(1996\)](#) as the ratio of the standard deviation of the reference data  
282 for the validation set to the RMSEP. The ideal model should have higher R and RPD  
283 values as well as lower RMSEC and RMSEP values. The optimal number of LVs was  
284 determined as the minimum number of LVs corresponding to the first lowest value of the  
285 RMSEC or RMSEP from the plot of the RMSEC or RMSEP for increasing number of  
286 LVs ([Davey et al. 2009](#)). The stability of the calibration model was tested by  
287 interchanging validation and calibration data sets and checking that the differences in the  
288 regression statistics obtained were small ([Alvarez-Guerra et al., 2010](#)).

289

### 290 **3. Results and discussion**

291

292 *3.1.Rind breakdown disorder and biochemical profile of fruit from different canopy*  
293 *positions.*

294

295 Symptoms of rind breakdown disorder were visible on affected fruit after five weeks of  
296 continuous storage at 8°C. RBD was significantly affected by preharvest manipulation of  
297 sunlight exposure ([Table 1](#)). Outside fruit had the lowest susceptibility to develop the  
298 disorder compared to other preharvest treatments. Fruit position within the canopy on its  
299 own did not show a significant difference on fruit susceptibility to RBD. However,  
300 exclusion of sunlight by bagging fruit resulted in increased fruit susceptibility but only  
301 showed a significant difference on fruit located inside the canopy. These findings are  
302 consistent with those observed by [Almela et al. \(1992\)](#). In their study, these authors  
303 established that the sensitivity of fruit to development of rind spots related to RBD in  
304 ‘Fortune’ mandarins was influenced by different microclimates. Similar to observations  
305 reported by [Cronje et al. \(2011\)](#), fruit position within the canopy affected rind colour  
306 index (CI). Fruit borne on the outside of the tree canopy had the highest CI and hence  
307 were more orange while shaded fruit had pale, yellow rinds.

308

309 Foregoing research suggests that rind water status is a factor prevailing in the  
310 susceptibility of citrus fruit to rind physiological disorders ([Cohen et al., 1994](#); [Alfárez](#)  
311 [and Burns \(2004\)](#)). In this study, fruit from the bagged treatments, both inside and outside  
312 of the canopy, were characterized by high postharvest weight loss, and this was  
313 essentially due to water loss by transpiration, as this account for 90% of total weight loss  
314 ([Ben-Yehoshua, 1969](#)). Water loss from the fruit results from a water pressure gradient

315 prevailing between the fruit rind, which is close to saturation with water, and the less  
316 saturated outer atmosphere (Ben-Yehoshua *et al.*, 1994; Macnish *et al.*, 1997).

317

318 Fruit position within the canopy also had a significant influence on rind biochemical  
319 properties. Results in **Table 1** showed that outside fruit had higher TSS, dry matter  
320 content, glucose and total phenolic acid concentrations compared to shaded samples. The  
321 effect of canopy position on fruit quality was documented by (Barry *et al.*, 2000) who  
322 reported that fruit from the south western top part of the canopy had significantly higher  
323 soluble solids contents, lower titratable acid content and higher ratio than fruit borne in  
324 the north east bottom position. In this study, bagged fruit from outer portion of the  
325 canopy had significantly higher glucose concentration of 92.03 mg/g DW compared to  
326 inside fruit, which had 66.92 mg/g DW glucose concentration. On the contrary, sucrose,  
327 and total carbohydrate of bagged fruit from inside the canopy were significantly higher in  
328 relation to other three positions. It was therefore noteworthy that these fruit also had  
329 highest susceptibility to RBD.

330

331 In addition to carbohydrate contents, phenolic acid concentration and antioxidant  
332 capacity were affected by fruit exposure to sunlight. Unbagged samples from the inside  
333 and outside position had relatively higher phenolic acid content of 39.29 and 37.65 mg/g  
334 DW when compared to outside bagged and inside bagged samples which had 33.48 and  
335 34.68 mg/g DW, respectively. Moreover, the antioxidant activity of inside bagged  
336 samples, i.e. fruit with the highest RBD, was much higher than those with low RBD  
337 disorder. It has reported previously that the presence antioxidant species or the lack

338 thereof could be implicated to the development of various postharvest disorders including  
339 non-chilling peel pitting in ‘Navelate’ oranges (Cajuste and Lafuente, 2007). The results  
340 presented above are in accord with the notion that manipulating light levels around an  
341 individual fruit reduces rind condition and susceptibility to the disorder. Pearson  
342 correlation analysis between physico-chemical properties and RBD development had  
343 very low correlation coefficients which serve to prove the complexity of factors involved  
344 in the development of this disorder. Furthermore, the lack of a specific threshold values  
345 below or above which all fruit become affected and above or below which all fruit stay  
346 healthy suggests that several preharvest and postharvest factors also play a role.

347

### 348 *3.2. Vis/NIR spectroscopy*

349

#### 350 *3.2.1. Distribution of prediction and validation reference data*

351

352 In this study, reference data set was partitioned into the calibration (60% of n) and  
353 validation (40% of n) set. **Table 2** shows the distributional statistics for reference datasets  
354 used in calibration and test validation. The reference measurements of all parameters in  
355 calibration and validation were fairly normally distributed round the means. Although the  
356 selection method for calibration and validation was random, validation data set was  
357 scrutinised to ensure that the validation data sets were confined within a boundary of the  
358 calibration set. The interpretation of calibration results depends greatly on the precision  
359 of the determined reference data and enough variation in both calibration and validation  
360 data (Lu et al. 2006). As is apparent in the range and CV% values of the data presented,



361 the calibration and validation values of the sample quality parameters cover a large range,  
362 which is helpful for developing calibration models for NIR spectroscopy (Clément et al.  
363 2008). For instance, the mean concentration of sucrose values used for calibration and  
364 validation were 101.40 and 78.81 mg/g DW with standard deviation of 43.27 and 34.15  
365 mg/g DW, respectively. The range of total sugars in the calibration set was from 121.91  
366 to 511.11 mg/g DW and the range of validation set was from 141.91 to 492.28 mg/g DW  
367 with corresponding CV % of 29.38 and 36.31%, respectively.

368

### 369 3.2.2. *Spectrum description*

370

371 The absorbance spectra presented in Figure 1(a) portrays the typical spectra obtained  
372 from intact “Nules Clementine” mandarins subjected to different preharvest treatments.  
373 Each line represents the average spectra from 20 fruit in each preharvest treatment.  
374 Spectral features were similar to those obtained by Gómez and co-workers (2006). Strong  
375 absorption bands around 670, 740, 980, 1200, 1450, 1780 and 1930 nm were observed.  
376 Absorption at these wavebands were, respectively, due to red absorbing pigments,  
377 particularly chlorophyll (Clément et al. 2008), third overtone of O-H stretching, second  
378 overtone of H-O-H stretching modes of water, second and first overtones of C-H  
379 stretching as well as the third overtone of O-H, C-H and C-H<sub>2</sub> deformation associated  
380 with sugar solution reported by Kawano et al. (1993) and Golic et al. (2003). It should be  
381 noted that the average spectra of inside bagged fruit (with highest RBD) had a distinctly  
382 stronger absorbance in the waveband between 600 and 900 nm. This was similar to  
383 results obtained by Zheng et al. (2010) for prediction of olleocellosis disorder, where large

384 variations in absorbance spectra were observed among fruit with different sensitivities in  
385 the same waveband. Since the intensities of reflectance vary with concentrations of  
386 biochemical constituents of the sample (Williams and Norris, 2001) this band may  
387 possibly be related to fruit sensitivity to rind physiological disorders such as oleocellosis  
388 and RBD.

389

### 390 3.2.3. *Pre-processing methods*

391

392 The spectra of solid samples such as fruit are influenced by physical properties such as  
393 shape, size, path length, etc. (Leonardi and Burns 1999), which create noise and  
394 determine light scattering properties. As a common practice in NIRS, obtained spectra  
395 was subjected to several pre-processing methods and the suitable pre-processing methods  
396 were selected. Results presented in Table 3 show that Savitzky-Golay second derivative  
397 with the fifth order polynomial (Figure 1(b)) provided the best results for the PCA  
398 classification and PLS model for predicting RBD. MSC (Figure 1(c)) gave best results for  
399 PLS prediction of physico-chemical properties such as  $h^{\circ}$ , CI, weight loss, dry matter  
400 content, and carbohydrate concentrations as well PLS-DA classification by preharvest  
401 treatments.

402

### 403 3.2.4. *Vis/NIR- based PCA and PLS classification models*

404

405 Individual spectra from 8 positions within the fruit and the average spectra were tested to  
406 develop PCA and PLD-DA classification models. Average spectra showed better models  
407 than individual spectra; and thus subsequent analyses were based on average spectra.

408 PCA was performed on Vis/NIR spectra to compare spectral characteristics of fruit from  
409 different preharvest treatments. The PCA applied to the spectra using Savitzky Golay  
410 second derivative pre-processing revealed better grouping of the samples than other  
411 tested pre-processing methods. The data distribution in the PCA score plot presented in  
412 **Figure 2** displayed four clusters that could easily be identified. These clusters allowed  
413 distinction between fruit from different preharvest treatments. The first two principal  
414 components (PC) accounted for 68.0 % of the total variability, PC1 explains the 53.0 %  
415 of the variance and PC2 explained 15.0 % of the variance. The effective wavelength band  
416 for this classification was from 350 to 1200 nm with a strong absorption at 670 nm  
417 influenced by chlorophyll and three at 740, 980, 1200 nm corresponding to water (O-H)  
418 functional groups. From this, it could be concluded that a combination of colour and  
419 moisture content of the rind play an important role in discriminating from different  
420 positions of the canopy.

421

422 Spectral data was further subjected to discriminant analysis by assigning fruit from each  
423 canopy positions to a dummy variable (1, 2, 3 and 4 for outside, outside bagged, inside  
424 bagged and inside, respectively). **Figure 3** depicts performance of the PLS-DA model to  
425 classify fruit based on their origin within the tree canopy using full spectral range (350-  
426 2500 nm) and MSC spectral pre-processing. The prediction accuracy determined using 24  
427 test set for validation was high ( $r = 0.971$ ,  $RMSEP = 0.304$ ).

428

429 *3.2.5. Vis/NIR- based PLS prediction models*

430

431 **Table 3** shows summary statistics for calibration and validation results for the prediction  
432 of different physico-chemical properties with PLS models. After testing different  
433 wavelength ranges based on observed peaks and information provided in the literature,  
434 wavelength bands that gave the lowest RMSEC and RMSEP were selected to develop  
435 calibration models for each physico-chemical property. As would be expected, models  
436 for colour parameters ( $h^\circ$  and CI) were developed using visible range (350-700 nm) of  
437 the spectrum, whereas RBD model was developed with the region between 350-1000 nm.  
438 This was in accordance with the range used by [Zheng et al. \(2010\)](#) to develop models for  
439 predicting susceptibility of citrus fruit to oleocellosis, another rind physiological disorder.

440

441 Prediction models for sucrose, fructose, glucose, total sugars, TSS, dry matter and water  
442 loss were developed using wavelength range between 900 to 1800 nm. According to the  
443 absorption bands of common foods constituents provided by [Williams and Norris \(2001\)](#),  
444 all these biochemical components have absorption bands in this spectral region. Results  
445 obtained in this study are similar to previous studies suggesting that the range from 350-  
446 1800 nm is suitable for predicting colour parameters ([Sun et al., 2009](#)), dry matter  
447 ([Guthrie et al., 2005a, b](#)), sucrose, fructose, glucose ([Tewari et al., 2008](#)) and sugar  
448 content ([Liu et al., 2010](#)).

449

450 Models for predicting quality parameters such as colour index,  $h^\circ$ , DM and water loss  
451 showed significantly high performance, with predictive  $R$  values ranging from 0.91 to  
452 0.98 and RPD ranging from 2.34 to 4.13 for water loss and CI, respectively (**Figure 5**).  
453 NIR calibration and validation results demonstrated that sugars, dry matter, colour index

454 and mass loss were predicted with significant accuracy. The prediction performance for  
455 sugars (sucrose, fructose, glucose, and total sugars) was high with  $R$  of 0.88, 0.94, 0.95,  
456 and 0.95 and corresponding RMSEP values of 24.36, 11.41, 11.58, 31.04 mg/g DW,  
457 respectively (Figure 6). Although the accuracy is slightly lower, these results were  
458 comparable to those reported in the literature by Tewari et al. (2008) for the prediction of  
459 sucrose, fructose and glucose of grapefruit.

460

461 As suggested by Davey et al. (2009) and Saeys et al. (2005), although the correlation  
462 between NIR predicted and reference values is high, it is also very critical to verify the  
463 accuracy of the model by referring to the RPD values. These authors stated that RPD  
464 values below 1.5 are considered unusable, those between 1.5 and 2.0 are suitable for  
465 rough prediction, those between 2.0 and 2.5 are suitable for quantitative predictions,  
466 while RPD values between 2.5 and above 3.0 are respectively considered good and  
467 excellent prediction models. The low RPD values, 0.30 and 1.40 for RBD and sucrose,  
468 respectively, clearly indicate poor accuracy of these models. The poor accuracy of these  
469 models could be attributed to high variation of these parameters in both calibration and  
470 test set data. Furthermore, the low predictability of sucrose could possibly results due to  
471 the difference in molecular weight of sucrose (MW=342.30 g/mol) compared to fructose  
472 and glucose (MW=180.16) (Golic et al., 2003). This difference in molecular weight is  
473 such that there are 1.89 times fewer number of sucrose molecules than glucose and  
474 fructose in the same weight of sample. Therefore, the intensity of the bands associated  
475 with hydrogen bonding is smaller in sucrose than in glucose and fructose.

476

477 The complexity of biological factors involved in the development of RBD complicated  
478 the development of an acceptable model for predicting the disorder. However, the high  
479 ability of Vis/NIR to classify fruit based on their origin within the canopy using PLS-DA  
480 could have online practical interest for online application. Another reason for the poor  
481 prediction model for RBD is that calibration and test set also contained a large proportion  
482 of samples in which RBD didn't develop. The inability to generate the disorder due to  
483 unfavourable conditions to develop the disorder under this type of study occurs. To correct  
484 this problem in future studies, it will be necessary to increase sample size for both calibration  
485 and validation sets. This is to ensure that the distribution of the disorder is wide, normal  
486 around the mean and that it represents distribution present in a harvested population of  
487 mandarin fruit (Davey et al. 2009).

488

#### 489 **4. Conclusions**

490

491 In this study, the positional effects within the canopy and bagging were significant in  
492 altering rind biochemical properties. Outside unbagged fruit had higher rind sugar,  
493 phenolic acids and dry matter content and lower RBD index than inside and bagged fruit.  
494 The data distribution in the PCA and PLS-DA models displayed four clusters that could  
495 easily be identified. These clusters allowed distinction between fruit from different  
496 preharvest treatments. NIR calibration and validation results demonstrated that sugars,  
497 dry matter, colour index and mass loss were predicted with significant accuracy. The  
498 exploration of the statistics of the developed models revealed the high potential that  
499 Vis/NIR spectroscopy has to non-destructively detect rind biochemical profile and hence  
500 susceptibility to RBD. The good correlation between spectral information and

501 biochemical information demonstrated the potential of Vis/NIR as a non-destructive tool  
502 to predict fruit susceptibility to RBD.

503

#### 504 **Acknowledgement**

505

506 This work is based upon research supported by the South African Research Chairs  
507 Initiative of the Department of Science and Technology and National Research  
508 Foundation. The authors are grateful to the South African Perishable Products Export  
509 Control Board (PPECB) and the South Africa/Flanders Research Cooperation  
510 Programme (Project UID: 73936) for financial support which made it possible to  
511 undertake the study, and to Rosemary Burns and Kate Cools for technical research  
512 support. Mr Lembe Magwaza's study visit at Cranfield University was partly funded by  
513 the Commonwealth Scholarship Commission of the United Kingdom.

514

#### 515 **References**

516

- 517 [Agustí, M., Almela, V., Juan, M., Alférez, F., Tadeo, F.R., Zacarias, L., 2001.](#)  
518 [Histological and physiological characterisation of rind breakdown of 'Navelate'](#)  
519 [sweet orange. Ann. Bot. 88, 415–422.](#)
- 520 [Alférez, F., Zacarias, L., 2001. Postharvest pitting in navel oranges at non-chilling](#)  
521 [temperature: Influence of relative humidity. Acta Hort. 553, 307–308 .](#)

522 Alférez, F., Burns, J., 2004. Postharvest peel pitting at non-chilling temperatures in  
523 grapefruit is promoted by changes from low to high relative humidity during  
524 storage. *Postharvest Biol. Technol.* 32, 79–87.

525 Alférez, F., Agustí, M., Zacarias, L., 2003. Postharvest rind staining in ‘Navel’ oranges is  
526 aggravated by changes in storage relative humidity: effect on respiration, ethylene  
527 production and water potential. *Postharvest Biol. Technol.* 28, 143–152.

528 Almela, V., Agustí, M., Pons, J., 1992. Rind spots in ‘Fortune’ mandarin. Origin and  
529 control. *Physiol. Plant.* 85, A65 (Abstract).

530 Alvarez-Guerra, M., Ballabio, D., Amigo, J.M., Bro, R., Viguri, J.R., 2010. Development  
531 of models for predicting toxicity from sediment chemistry by partial least squares-  
532 discriminant analysis and counter-propagation artificial neural networks.  
533 *Environ. Pollut.* 158, 607–614.

534 Barry, G.H., Castle, M.S., Davies, F.S., 2000. Juice quality of ‘Valencia’ sweet orange  
535 among citrus-producing regions in Florida and between canopy positions. *Proc.*  
536 *Int. Soc. Citricult. Congr. IX*, 308–314.

537 Barry, G.H., Rabe, E., 2004. Clementine mandarin production in South Africa. *Proc. Intl.*  
538 *Soc. Citricult. Congr. I*, 360–363.

539 Ben-Yehoshua, S. 1969. Gas exchange, transpiration, and the commercial deterioration in  
540 storage of orange fruit. *J. Am. Soc. Hortic. Sci.* 94, 524–528.

541 Ben-Yehoshua, S., Shapiro, B., Chen, Z.E., Lurie, S., 1983. Mode of action of plastic  
542 film in extending life of lemon and bell pepper fruits by alleviation of water  
543 stress. *Plant Physiol.* 73, 87–93.



544 Blasco, J., Aleixos, N., Moltó, E., 2007. Computer vision detection of peel defects in  
545 citrus by means of a region oriented segmentation algorithm. *J. Food Eng.* 81,  
546 535–543.

547 Butz, P., Hofmann, C., Tauscher, B., 2005. Recent developments in non-invasive  
548 techniques for fresh fruit and vegetable internal quality analysis. *Concise Rev.*  
549 *Food Sci.* 70, 131–141.

550 Cajuste, J.F., Lafuente, T.M., 2007. Ethylene-induced tolerance to non-chilling peel  
551 pitting as related to phenolic metabolism and lignin content in ‘Navelate’ fruit.  
552 *Postharvest Biol. Technol.* 45, 193–203.

553 Chen, X., Wu, D., He, Y., Liu, S., 2011. Nondestructive differentiation of *Panax* species  
554 using visible and shortwave near-infrared spectroscopy. *Food Bioprocess*  
555 *Technol.* 4, 753–761.

556 Chikaizumi, S., 2000. Mechanism of rind-oil spot development in ‘Encore’ (*Citrus*  
557 *nobilis* Lour. X *C. Deliciosa* Ten.) fruit. *J. Jpn. Soc. Hortic. Sci.* 69, 149–155.

558 Clark, C.J., McGlone, V.A., DeSilva, H.N., Manning, M.A., Burdon, J., Mowat, A.D.,  
559 2004. Prediction of storage disorders of kiwifruit (*Actinidia chinensis*) based on  
560 visible-NIR spectral characteristics at harvest. *Postharvest Biol. Technol.* 32,  
561 147–158.

562 Clément, A., Dorais, M., Vernon, M., 2008. Nondestructive measurement of fresh tomato  
563 lycopene content and other physicochemical characteristics using visible-NIR  
564 spectroscopy. *J. Agric. Food Chem.* 56, 9813–9818.

565 Cohen, E., Shapiro, B., Shalom, Y., Klein, J.D., 1994. Water loss: A non-destructive  
566 indicator of enhanced cell membrane permeability of chilling-injured citrus fruit.  
567 J. Am. Soc. Hortic. Sci. 119, 983–986.

568 Crespo, P., Giné Bordonaba, J., Terry, L.A., Carlen, C., 2010. Characterisation of major  
569 taste and health-related compounds of four strawberry genotypes grown at  
570 different Swiss production sites. Food Chem. 122, 6–24.

571 Cronje, P.J.R., 2005. Peteca spot of lemons. S. Afr. Fruit J. Feb/March, 26–28.

572 Cronje, P.J.R., 2007. Postharvest rind disorders of citrus fruit. Citrus research  
573 international, Nelspruit, South Africa.

574 Cronje, P.J.R., 2009. Postharvest rind breakdown of ‘Nules Clementines’ mandarins  
575 (*Citrus reticulata* Blanco) fruit. PhD Dissertation, University of Stellenbosch,  
576 Stellenbosch, South Africa.

577 Cronje, P.J.R., Barry, G.H, Huysamer, M., 2011. Postharvest rind breakdown of ‘Nules  
578 Clementine’ mandarin is influenced by ethylene application, storage temperature  
579 and storage duration. Postharvest Biol. Technol. 60, 192–201.

580 Davey, M.W., Saeys, W., Hof, E., Ramon, H., Swennen, R.L., Keulemans, J., 2009.  
581 Application of visible and near-infrared reflectance spectroscopy (Vis/NIRS) to  
582 determine carotenoid contents in banana (*Musa* spp.) fruit pulp. J. Agric. Food  
583 Chem. 57, 1742–1751.

584 Duarte, A.M.M., Guardiola, J.L., 1995. Factors affecting rind pitting in the mandarin  
585 hybrids ‘Fortune’ and ‘Nova’. The influence of exogenous growth regulators.  
586 Acta Hortic. 379, 59–67.

587 Geeola, F., Geeola, F., Peiper, U.M., 1994. A spectrophotometric method for detecting  
588 surface bruises on ‘Golden Delicious’ apples. *J. Agric. Eng. Res.* 58, 47–51.

589 Giné Bordonaba, J., Terry, L.A. 2008. Biochemical profiling and chemometric analysis  
590 of seventeen UK-grown black currant cultivars. *J. Agric. Food Chem.* 56, 7422–  
591 7430.

592 Golic, M., Walsh, K.B., Lawson, P., 2003. Short-wavelength near-infrared spectra of  
593 sucrose, glucose, and fructose with respect to sugar concentration and  
594 temperature. *Appl. Spectrosc.* 57, 139–145.

595 Gómez, A.H., He, Y., Pereira, A.G., 2006. Non-destructive measurement of acidity,  
596 soluble solids and firmness of Satsuma mandarin using Vis-NIR spectroscopy  
597 techniques. *J. Food Eng.* 77, 313–319.

598 Guthrie, J.A., Walsh, K.B., Reid, D.J., Liebenberg, C.J., 2005a. Assessment of internal  
599 quality attributes of mandarin fruit. 1. NIR calibration model development. *Aust.*  
600 *J. Agric. Res.* 56, 405–416.

601 Guthrie, J.A., Reid, D.J., Walsh, K.B., 2005b. Assessment of internal quality attributes of  
602 mandarin fruit. 2. NIR calibration model robustness. *Aust. J. Agric. Res.* 56, 417–  
603 426.

604 Jimenez-Cuesta, M., Cuquerella, J., Martínez-Jávega, J.M., (1981). Determination of a  
605 colour index for citrus degreening. *Proc. Int. Soc. Citricult.* 2, 750–753.

606 Kawano, S., Fujiwara, T., Iwamoto, M., 1993. Non-destructive determination of sugar  
607 content in ‘Satsuma’ mandarins using NIRS transmittance. *J. Jpn. Soc. Hortic.*  
608 *Sci.* 62, 465–470.

609 Khumalo, N.P., 2006. Factors affecting post-storage quality of ‘Nules Clementine’  
610 mandarin fruit with special reference to rind breakdown. MSc Thesis, University  
611 of Stellenbosch.

612 Kuang B., Mouazen, A.M., 2011. Calibration of visible and near infrared spectroscopy  
613 for soil analysis at the field scale on three European farms. *Eur. J. Soil Sci.* 62,  
614 629–636.

615 Lafuente, M.T., Sala, J.M., 2002. Abscisic acid levels and the influence of ethylene,  
616 humidity and storage temperature on the incidence of postharvest rindstaining of  
617 ‘Navelina’ orange (*Citrus sinensis* L. Osbeck) fruit. *Postharvest Biol. Technol.*  
618 25, 49–57.

619 Lafuente, M.T., Martínez-Téllez, M.A. and Zacarías, L. (1997). Abscisic acid in the  
620 response of ‘Fortune’ mandarins to chilling, effects of maturity and high-  
621 temperature conditioning. *J. Sci. Food Agric.* 73, 494–502.

622 Landahl, S., Meyer, M.D., Terry, L.A., 2009. Spatial and temporal analysis of textural  
623 and biochemical changes of imported avocado cv. ‘Hass’ during fruit ripening. *J.*  
624 *Agricult. Food Chem.* 57, 7039–7047.

625 Leonardi, L., Burns, D.H., 1999. Quantitative multiwavelength constituent measurements  
626 using single-wavelength photo time-of-flight correction. *Appl. Spectrosc.* 53,  
627 637–646.

628 Liu, Y., Sun, X., Ouyang, A., 2010. Non-destructive measurements of soluble solid  
629 content of navel orange fruit by visible-NIR spectrometric technique with PLSR  
630 and PCA-BPNN. *LWT:Food Sci. Technol.* 43, 602–607.

631 Lu, H., Xu, H., Ying, Y., Fu, X., Yu, H., & Tian, H. (2006). Application of Fourier  
632 transform near infrared spectrometer in rapid estimation of soluble solids content  
633 of intact citrus fruits. *Journal of Zhejiang University Science*, 7, 794-799.

634 Macnish, A.J. Joyce, D. C., Hetherington, S.E., 1997. Packaging to reduce water loss can  
635 delay ripening of mango (*Mangifera indica* L. cv. 'Kensington Pride') fruit. *Aust.*  
636 *J. Exp. Agric.* 37, 463–467.

637 Magwaza, L.S., Opara, U.L., Nieuwoudt, H., Cronje, P., 2011. NIR spectroscopy  
638 applications for internal and external quality analysis of citrus fruit – a review.  
639 *Food Bioprocess Technol.* DOI: 10.1007/s11947-011-0697-1.

640 Miller, B.K., Delwiche, M.J., 1991. Spectral analysis of peach surface defects. *Trans.*  
641 *Am. Soc. Agric. Eng.* 34, 2509-2515.

642 Peiris, K.H.S., Dull, G.G., Leffler, R.G., 1998. Nondestructive detection of selection  
643 drying, an internal disorder in tangerine. *HortSci.* 33, 310–312.

644 Saeys, W., Mouazen, A.M., Ramon, H., 2005. Potential onsite and online analysis of pig  
645 manure using visible and near infrared reflectance spectroscopy. *Biosyst. Eng.* 91,  
646 393–402.

647 Sun, X., Zhang, H., Liu, Y., 2009. Nondestructive assessment of quality of 'Nanfeng'  
648 mandarin fruit by a portable near infrared spectroscopy. *Int. J. Agric. Biol. Eng.* 2,  
649 65–71.

650 Teerachaichayut, S., Terdwongworakul, A., Thanapese, W., Kiji, K., 2011. Non-  
651 destructive prediction of hardening pericarp disorder in intact mangosteen by near  
652 infrared transmittance spectroscopy. *J. Food Eng.* 106, 206–211.

653 Terry, L.A., Chope, G.A., Giné Bordonaba, J., 2007. Effect of water deficit irrigation and  
654 inoculation with *Botrytis cinerea* on strawberry (*Fragaria x ananassa*) fruit  
655 quality. J. Agric. Food Chem. 55, 10812–10819.

656 Tewari, J.C., Dixit, V., Chi, B-K., Malik, K.A., 2008. Determination of origin and sugars  
657 of citrus fruit using genetic algorithm, correspondence analysis and partial least  
658 square combined with fiber optic NIR spectroscopy. Spectroc. Acta Part A: Mol.  
659 Biomol. Spectrosc. 71, 1119–1127.

660 Wild, B.L., 1991. Postharvest factors governing the development of peteca spot on  
661 ‘Meyer’ lemons. HortSci. 26, 287–289.

662 Williams, P., Norris, K.H., 2001. Variables affecting near infrared spectroscopic analysis.  
663 In: Williams, P., Norris, K.H. (Eds). Near Infrared Technology in the Agriculture  
664 and Food Industries, 2<sup>nd</sup> ed. The American Association of Cereal Chemists, St.  
665 Paul, MNL, pp. 171-185.

666 Williams, P.C., Sobering, D.C., 1996. How do we do it: a brief summary of the methods  
667 we use in developing near infrared calibrations. In: Davies AMC, Williams, P.  
668 (ed.). Near Infrared Spectroscopy: The future waves. Proc. 7th Internatl. Conf.  
669 Near Infra. Spectrosc. Montreal, Chichester, UK, pp. 185-188.

670 Zheng, Y., He, S., Yi, S., Zhou, Z., Mao, S., Zhao, X., Deng, L., 2010. Predicting  
671 oleocellosis sensitivity in citrus using Vis-NIR reflectance spectroscopy. Sci.  
672 Hortic. 125, 401–405.

673

674

675

676 **Table 1:** Physico-chemical profile of fruit from different canopy positions. Different  
 677 alphabets next to figures (mean and standard error of the mean) in the same row are  
 678 significantly different.

Quality Parameter	Canopy position			
	Outside	Outside bagged	Inside	Inside bagged
h°	67.34±0.58ns	75.50±1.46ns	62.94±11.32ns	74.01±0.97ns
CI	6.12±0.19b	3.62±0.38a	3.65±0.57a	3.99±0.27a
Mass (g)	107.63±4.68b	104.89±4.28b	89.29±4.95a	107.61±6.38b
RBDI	0.00±0.00a	0.05±0.03a	0.04±0.04a	0.19±0.05b
WL (g)	9.51±0.42ab	13.02±1.76bc	7.76±0.58a	13.62±1.67c
TSS (°Brix)	13.71±0.24b	11.89±0.28a	12.11±0.27a	11.94±0.25a
DMC (%)	30.00±0.78b	26.98±0.51a	28.78±0.96a	26.99±0.79ab
Sucrose (mg/g DW)	95.31±6.07b	93.59±9.51b	63.30±8.65a	114.94±12.51b
Glucose (mg/g DW)	92.03±5.29b	85.44±8.94ab	66.92±6.97a	77.09±8.50ab
Fructose (mg/g DW)	126.48±5.19ab	130.21±9.76b	100.65±8.52a	122.26±9.71ab
Total Sugars (mg/g DW)	313.82±11.58b	309.23±25.05b	230.88±22.82a	314.29±27.70b
Total phenolic acids (mg/g DW)	39.29±0.86b	33.48±1.10a	37.65±0.85b	34.68±1.25a
DPPH (µmol trolox eq./g DW)	0.95±0.04b	1.23±0.18b	0.50±0.11a	1.36±0.17b

679

680

681

682

683

684

685

686

687 **Table 2:** Mean, standard deviation (SD), range and coefficient of variation (CV %) for  
 688 calibration (60% of n) and validation (40% of n) subsets of mandarin fruit.

Quality parameter	Calibration data set			Validation data set		
	Mean±SD	Range	CV%	Mean±SD	Range	CV%
h°	73.14±5.11	63.53-89.27	7.05%	72.28±6.27	64.51-85.71	8.54%
CI	4.52±1.47	1.25-7.49	32.59%	4.29±1.76	0.07-7.04	41.12%
RBDI	0.09±0.18	0.00-0.56	205.84%	0.05±0.10	0.00-0.33	187.75%
Mass (g)	107.90±22.87	67.40-153.60	21.20%	94.58±15.07	70.7-123.1	15.93%
WL (g)	11.33±5.21	4.51-28.53	45.99%	10.83±6.45	4.87-25.84	59.52%
DMC (%)	27.85±3.14	22.84-35.41	11.28%	28.56±3.29	23.54-35.71	11.50%
Sucrose (mg/g DW)	101.40±43.27	35.17-207.91	42.66%	78.81±34.15	42.85-144.30	43.34%
Glucose (mg/g DW)	83.87±30.11	22.19-152.1	35.91%	75.69±32.59	36.01-127.60	43.06%
Fructose (mg/g DW)	124.30±33.52	53.72-195.9	26.96%	114.70±37.38	59.38-182.48	32.62%
Total Sugars (mg/g DW)	309.60±90.97	121.91-511.11	29.38%	269.17±97.74	141.91-492.28	36.31%
PLS-DA dummy variables	2.34±1.07	1.00-4.00	45.79%	2.63±1.17	1.00-4.00	44.67%

689

690

691

692

693

694

695

696

697

698

699

700



701 Table 3: An overview of statistics obtained during calibration and validation of models  
 702 for individual quality parameters.

Quality parameter			Calibration model			Validation model			
	LV	Prepr	R	RMSEC	RPD	R	RMSEP	RPD	Info. Region (nm)
h°	3	MSC	0.97	1.31	3.91	0.97	1.66	3.78	350-700
CI	3	MSC	0.98	0.37	3.93	0.98	0.43	4.13	350-700
RBD (binary scores)	5	2nd der	0.77	0.27	0.67	0.70	0.34	0.30	350-1000
WL (g)	10	MSC	0.92	2.01	2.59	0.91	2.76	2.34	900-1700
DMC (%)	8	MSC	0.98	0.68	4.65	0.96	0.92	3.57	900-1700
Sucrose (mg/g DW)	10	MSC	0.96	12.38	3.50	0.88	24.36	1.40	900-1700
Glucose (mg/g DW)	10	MSC	0.95	9.18	3.28	0.94	11.41	2.86	900-1700
Fructose (mg/g DW)	14	MSC	0.98	6.33	5.30	0.95	11.58	3.23	900-1700
Total Sugars (mg/g DW)	10	MSC	0.94	30.42	2.99	0.95	31.04	3.15	900-1700
PLS-DA dummy variables	10	MSC	0.98	0.20	5.25	0.97	0.30	3.85	350-2500

703

704

705

706

707

708

709

710

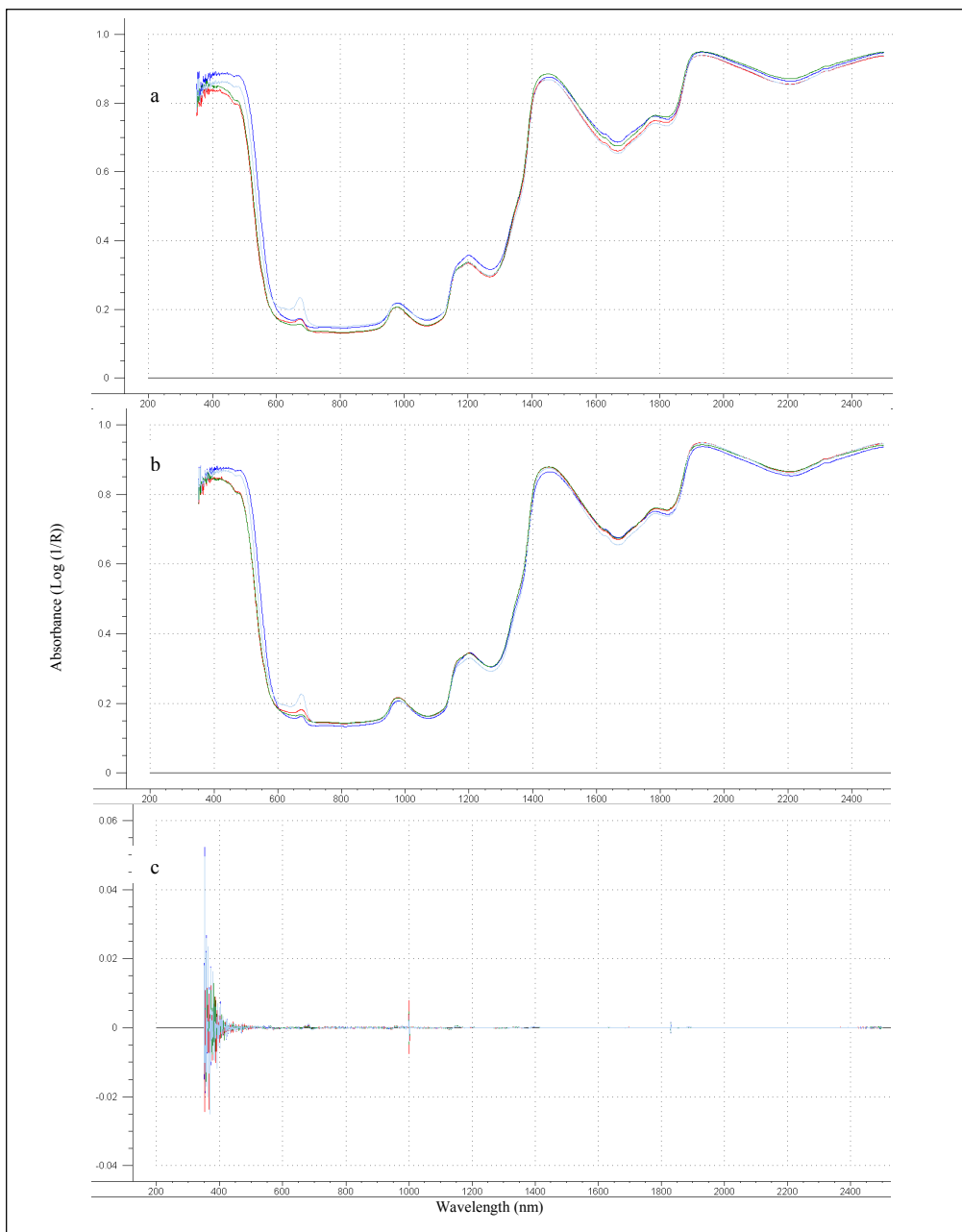
711

712

713

714

715  
716  
717  
718  
719  
720  
721  
722  
723  
724  
725  
726  
727  
728  
729  
730  
731  
732



733 **Figure 1:** Typical average Vis/NIR spectra (350-2500 nm) of intact “Nules Clementine”  
734 mandarins obtained from fruit harvested from four different preharvest treatments;  
735 outside (*deep blue line*), outside bagged (*red line*), inside (*inside*), and inside bagged  
736 (*light blue line*). (a) Without pre-processing; (b) multiple scatter correction; (c) Savitsky-  
737 Golay first derivative of the spectra.

738

739

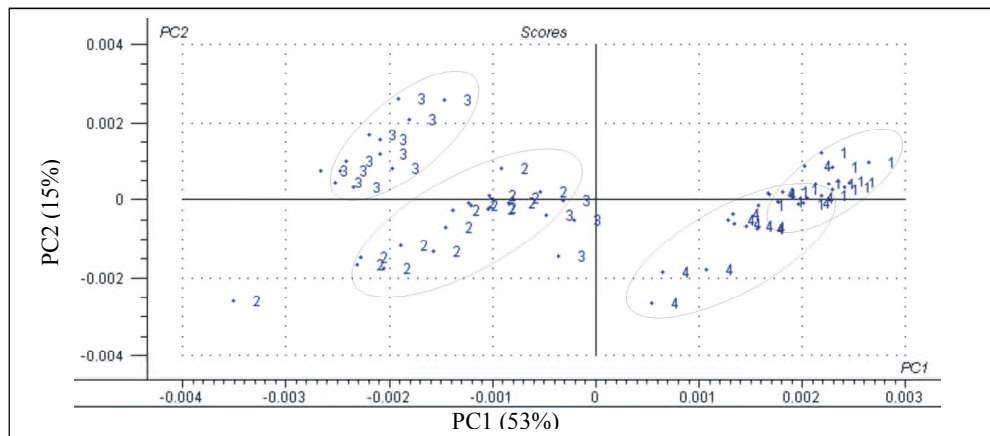
740

741

742

743

744



745

746 **Figure 2:** PCA plot for the two PC factors showing spectral ability to sort based on their

747 origin within the tree canopy.

748

749

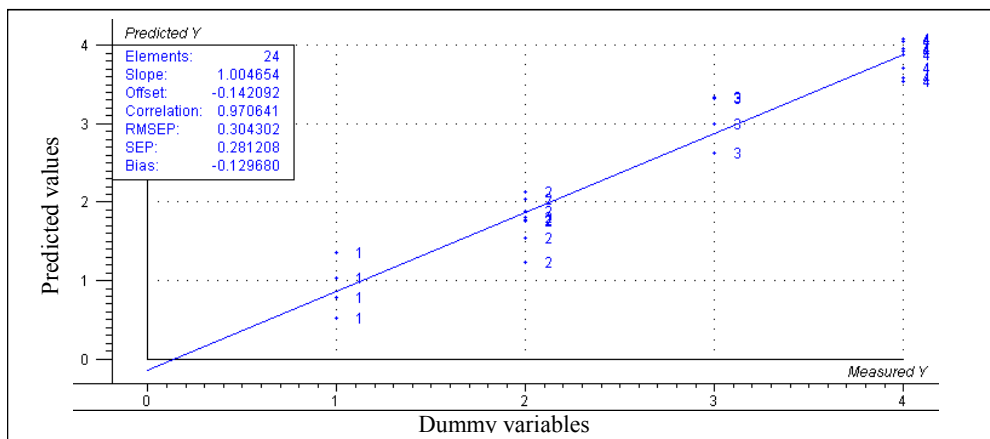
750

751

752

753

754



755

756 **Figure 3:** PLS-DA models showing Vis/NIR spectral ability to predict fruit origin within

757 the tree canopy.

758

759

760

761  
762  
763  
764  
765  
766  
767  
768  
769  
770  
771  
772  
773  
774  
775  
776  
777  
778  
779  
780  
781  
782  
783

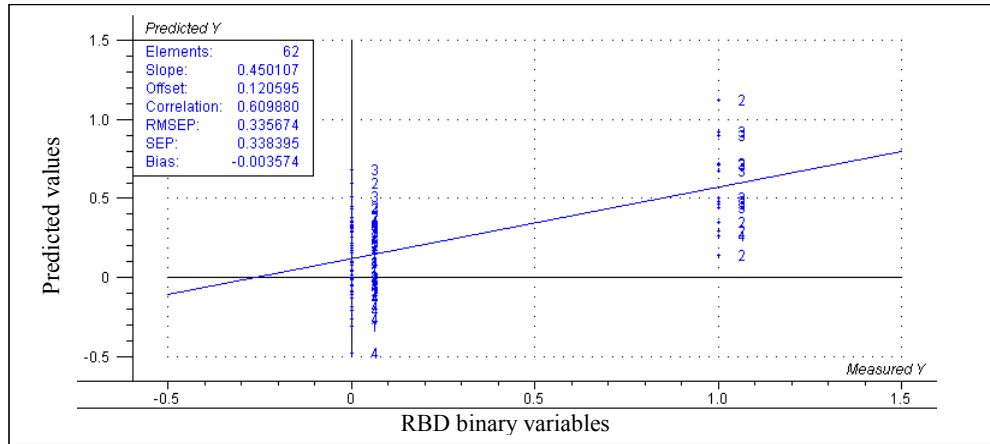


**Figure 4:** PLS scatter plot showing Vis/NIR model performance to classify fruit based on the occurrence of RBD.

784

785

786

787

788

789

790

791

792

793

794

795

796

797

798

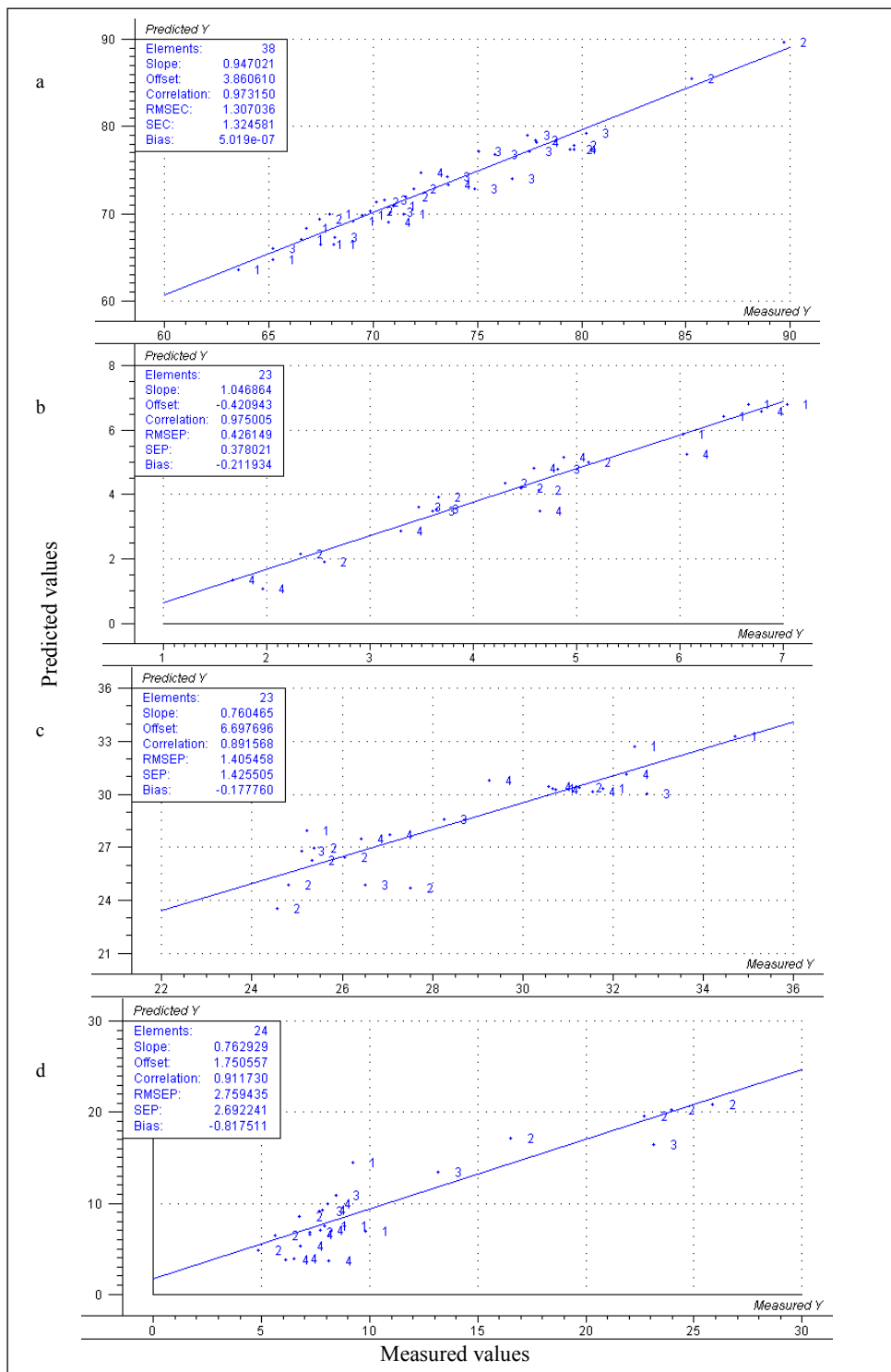
799

800

801

802

803

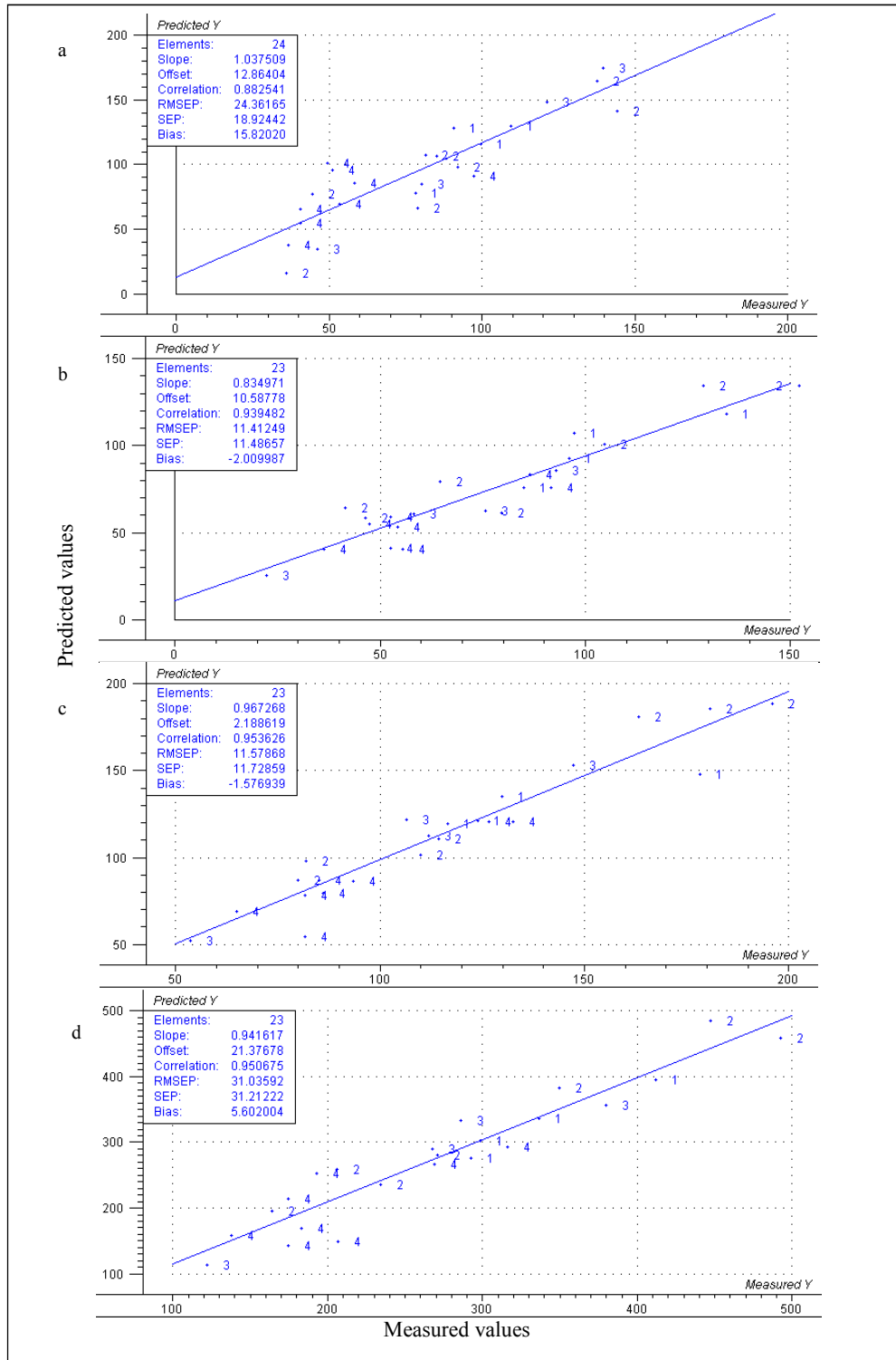


804 **Figure 5:** Scatter plots of Vis/NIR predicted versus measure values of hue angle (a),

805 colour index (b), dry matter (%) (c), and weight/water loss (grams) (d).

806

807  
 808  
 809  
 810  
 811  
 812  
 813  
 814  
 815  
 816  
 817  
 818  
 819  
 820  
 821  
 822  
 823  
 824  
 825  
 826  
 827



828 **Figure 6:** Scatter plots for Vis/NIR predicted versus measure values of sucrose (a),  
 829 glucose (b), fructose (c), and total sugars (d). All results are expressed in mg/g DW.